Two indenter interactions in analogue experiments - a further explanation of curved fold-and-thrust belts

Karsten Reiter[a,b], Nina Kukowski[b,c], Lothar Ratschbacher[a]

correspondence: reiter@gfz-potsdam.de

[a] TU Bergakademie Freiberg, Institute of Geology, Bernhard-v.-Cotta Str. 2, 09599 Freiberg, Germany
[b] GFZ German Research Centre for Geosciences, Telegrafenberg, 14473 Potsdam, Germany
[c] present address: Friedrich Schiller University of Jena, Institute of Geosciences, Burgweg 11, 07749 Jena, Germany

Curved fold-and-thrust belts mirror the deformation history of an orogenic belt and its foreland. Previous analogue experiments investigated the evolution of curved fold-and-thrust belts (Marshak and Wilkerson 1992, Calassou et al. 1993, Zweigel 1998, Macedo and Marshak 1999, Keep 2000, Cotton and Koyi 2000, Schreurs et al. 2001, Marques and Cobbold 2002, 2006), focusing on indenter shape, thickness variations within the deforming layers, detachment rheology and lateral changes of detachment rheology and width of the layer stack (see also Costa and Vendeville 2002, Couzens-Schultz et al. 2003).

A new approach with two indenters is tested as a further parameter in this study. Scaled analogue experiments are used to investigate the indentation of two basement blocks into a sedimentary basin and the formation of a curved fold-and-thrust belt. The experimental set-up has two flat indenters (same height as the layer cake); it permits the development of bivergent orogenic wedges (Byrne et al. 1988, Koons 1990, Bonini et al. 1999, Persson and Sokoutis 2002, Persson et al. 2004). A deformable "effective indenter" develops at the indenter front (Bonini et al. 1999, Persson and Sokoutis 2002) with a single back thrust that enables material to flow onto the indenter. The fast indenter have a width of 40 cm and the slow one of 60 cm, moving in parallel to each other, where the slow indenter has a relative velocity of 40–80 % of that of the fast indenter; both were pushed forward by thread rods driven by electrical motors (Fig. 1). All experiments were stopped after a FI convergence of 60 cm.

We modelled the sediments on top of the detachment by 15 mm thick dry quartz sand, a Mohr-Coulomb material with negligible cohesion and a linear stress-strain relationship up to failure (Byerlee 1978, Schellart 2000). The basal detachment is represented by 3 mm of low-friction glass beads (or 5 mm silicone oil in the second series). Given the 100×100 cm model size and the width of our indenters versus a natural analogue around 500 km basin width, we used a geometric scaling factor of 5×10^5 (i.e. 1 cm corresponds to 5 km).

We recorded the model run via 3D particle image velocimetry (3D-PIV; e.g. Hampel et al. 2004, Adam et al. 2005), employing a stereoscopic camera set-up with two 14 bit monochromatic Charge Coupled Device (CCD) cameras having a resolution of 11 million pixels. To optimise optical correlation, we mixed the sand with 8 % of black sand. Based on the recorded data, spatio-temporal topography (Fig. 2), displacement filed and strain distribution is calculated. In this study the accuracy of vectors

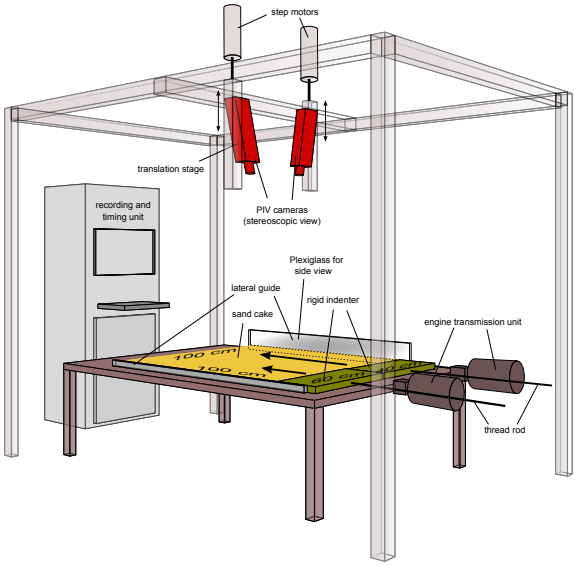

Figure 1: Sketch of the experimental set-up and PIV monitoring. The model has dimensions of 100×100 cm, the fast indenter is 40 cm wide, the slow one 60 cm. Both indenters are laterally guided and driven by two thread rods and engines. The experiments are recorded in stereoscopic view, to monitor the surface of the model in 3D via 3D particle image velocimetry.

(maximum measured displacement in static areas) is <0.02 mm in x- and y-direction (horizontal) and <0.05 mm in z-direction (topography). After each experimental run, the model was covered with black sand in order to stabilise structures and drizzled with ≈ 4.5 l water to reach saturation at a moisture of $\approx$25 Vol.% (pore space filled). Then, we cut vertical sections through the deformed layer cake to observe the internal structure.

During the experiments, a wedge evolves in front of the indenters by fore-thrusting according to the critical taper theory of Davis et al. (1983) and Dahlen et al. (1984). Thrusting wedge development in the transfer zone depends crucially on the relative velocity: When the slow indenter moves with a velocity of more than 55 % of the fast indenter, a single curved thrust wedge develops. The wedge becomes decoupled along a strike-slip zone at large velocity differences, i.e. when the slow indenter moves slower than 55 % of the fast indenter velocity. Consequently, the thrust front is strongly curved at high (55–60 %) and smoothly curved at low velocity differences (70–80 %); in all cases, curvature increases during indentation.

Along the most strongly curved portion of the thrust wedge, the transfer zone rises, particle rotation and material transport oblique to the indentation direction occur directed toward the front of the slow indenter. Thrusting cycles are timed by the fast indenter and influence thrusting in front of the slow indenter. Thrusts nucleate in front of the fast indenter wedge and propagate laterally to the slow indenter front. This implies distant effects of wedge growth are active hundreds of kilometre alongstrike of orogens. Such a thrust wedge in front of the SI, influenced by lateral fault propagation, grows faster in width, is slower in elevation growth, and has a smaller slope angle than one without lateral fault propagation. The thrust wedge is internally torn by a strike slip fault, parallel to the orientation of indentation, running from the orogenic wedge to the back thrust region atop the margin between both indenters, accommodating the different indenter velocities.

Several fold-and-thrust belts were formed by thin-skinned deformation atop a weak detachment (evaporites or layers with pore-fluid overpressure - e.g. Davis and Engelder 1985, Macedo and Marshak 1999). Rock salt has strain-rate dependent deformation behaviour with brittle failure occurring at high and viscous flow at low strain

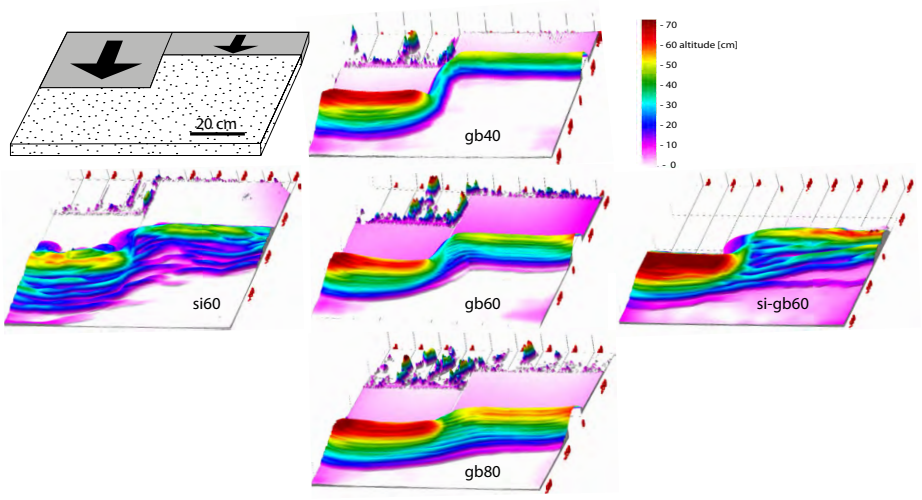

Figure 2: Thrust wedges in 3D view in the final stage after 60 cm fast indenter convergence of the 40 % (gb40), 60 % (gb60), and 80 % (gb80) experiments with glass beads detachment. The wedge of the 40 % experiment decouples in an early stage. The 60 % (gb60) model wedge is connected but strongly curved, whereas the 80 % experiment has a smoothly curved wedge. The experiments with 60 % relative velocity and the detachment made of silicone oil (si60) or of glass beads in front of the fast indenter and the silicone oil in front of the slow indenter (si-gb60) display the influence of the detachment rheology on the surface deformation. The length of a wedge is about 100 cm, the surface is colour coded according to height. The steep topography behind the indenters is an artefact of lost optical correlation. Set-up sketch in the upper left corner.

rates. We used silicone oil to model a viscous detachment in the second experimental series. The viscous behaviour requires proper scaling for velocity (Hubbert 1937, Weijermars and Schmeling 1986): Viscosities of evaporitic rocks are in a range of 10^{17} to 10^{19} Pa s (Clark 1966 cited in Couzens-Schultz et al. 2003, Cotton and Koyi 2000). Used convergence rates of 2 cm/h in the model equates typical convergence rates in nature (1.5 cm/yr).

The 60 % experiment with the viscous detachment is less curved compared to the experiment with the same velocity ratio and a glass beads detachment (si60 versus gb60 in Fig. 2). Deformation atop of silicone oil is more irregular and buckled onto the glass beads. Silicone oil permits variable thrust vergence with fore- and backthrusts within the pro-wedge; the wedges has a lower angle than those with glass beads, because of different basal friction. When a viscous detachment in front of the slow indenter occurs in the foreland, together with a frictional detachment in the fast indenter foreland, a nearly straight thrust front occurs (si-gb60 in Fig. 2). But thrust orientation changes laterally depending on the detachment rheology.

References

Adam, J., Urai, J. L., Wieneke, B., Oncken, O., Pfeiffer, K., Kukowski, N., Lohrmann, J., Hoth, S., van der Zee, W. and Schmatz, J.: 2005, Shear localisation and strain distribution during tectonic faulting — new insights from granular-flow experiments and high-resolution optical image correlation techniques, *Journal of Structural Geology* **27**(2), 283–301.

Bonini, M., Sokoutis, D., Talbot, C. J., Boccaletti, M. and Milnes, A. G.: 1999, Indenter growth in analogue models of Alpine-type deformation, *Tectonics* **18**(1), 119–128.

Byerlee, J.: 1978, Friction of rocks, *Pure and Applied Geophysics* **116**(4-5), 615–626.

Byrne, D. E., Davis, D. M. and Sykes, L. R.: 1988, Loci and maximum size of thrust earthquakes and the mechanics of the shallow region of subduction zones, *Tectonics* **7**(4), 833–857.

Calassou, S., Larroque, C. and Malavieille, J.: 1993, Transfer zones of deformation in thrust wedges: an experimental study, *Tectonophysics* **221**(3-4), 325–344.

Clark, G. B.: 1966, Deformation moduli of rocks, *ASTM Special Technical Publication* **402**, 133–172.

Costa, E. and Vendeville, B. C.: 2002, Experimental insights on the geometry and kinematics of fold-and-thrust belts above weak, viscous evaporitic décollement, *Journal of Structural Geology* **24**(11), 1729–1739.

Cotton, J. T. and Koyi, H. A.: 2000, Modeling of thrust fronts above ductile and frictional detachments: Application to structures in the Salt Range and Potwar Plateau, Pakistan, *Geological Society of America Bulletin* **112**(3), 351–363.

Couzens-Schultz, B. A., Vendeville, B. C. and Wiltschko, D. V.: 2003, Duplex style and triangle zone formation: insights from physical modeling, *Journal of Structural Geology* **25**(10), 1623–1644.

Dahlen, F. A., Davis, D. and Suppe, J. a.: 1984, Mechanics of fold-and-thrust belts and accretionary wedges: cohesive Coulomb theory, *Journal of Geophysical Research* **89**(B12), 10,087–10,101.

Davis, D. M. and Engelder, T.: 1985, The role of salt in fold-and-thrust belts, *Tectonophysics* **119**(1-4), 67–88.

Davis, D., Suppe, J. and Dahlen, F. A.: 1983, Mechanics of fold-and-thrust belts and accretionary wedges, *Journal of Geophysical Research* **88**(B2), 1153–1172.

Hampel, A., Adam, J. and Kukowski, N.: 2004, Response of the tectonically erosive south Peruvian Forearc to subduction of the Nazca Ridge: Analysis of three-dimensional analogue experiments, *Tectonics* **23**(5), 16.

Hubbert, M. K.: 1937, Theory of scale models as applied to the study of geologic structures, *Bulletin of the Geological Society of America* **48**(10), 1459–1520.

Keep, M.: 2000, Models of lithospheric-scale deformation during plate collision: effects of indentor shape and lithospheric thickness, *Tectonophysics* **326**(3-4), 203–216.

Koons, P. O.: 1990, Two-sided orogen: collision and erosion from the sandbox to the Southern Alps, New Zealand, *Geology (Boulder)* **18**(8), 679–682.

Macedo, J. and Marshak, S.: 1999, Controls on the geometry of fold-thrust belt salients, *Geological Society of America Bulletin* **111**(12), 1808–1822.

Marques, F. O. and Cobbold, P. R.: 2002, Topography as a major factor in the development of arcuate thrust belts: insights from sandbox experiments, *Tectonophysics* **348**(4), 247–268.

Marques, F. O. and Cobbold, P. R.: 2006, Effects of topography on the curvature of fold and thrust belts during shortening of a 2-layer model of continental lithosphere, *Tectonophysics* **415**(1-4), 65–80.

Marshak, S. and Wilkerson, M. S.: 1992, Effect of overburden thickness on thrust belt geometry and development, *Tectonics* **11**(3), 560–566.

Persson, K. S., Garcia-Castellanos, D. and Sokoutis, D.: 2004, River transport effects on compressional belts: First results from an integrated analogue-numerical model, *Journal of Geophysical Research* **109**(B1), 1–11.

Persson, K. S. and Sokoutis, D.: 2002, Analogue models of orogenic wedges controlled by erosion, *Tectonophysics* **356**(4), 323–336.

Schellart, W. P.: 2000, Shear test results for cohesion and friction coefficients for different granular materials: scaling implications for their usage in analogue modelling, *Tectonophysics* **324**(1-2), 1–16.

Schreurs, G., Haenni, R. and Vock, P.: 2001, Four-dimensional analysis of analog models; experiments on transfer zones in fold and thrust belts, *Memoir - Geological Society of America* **193**, 179–190.

Weijermars, R. and Schmeling, H.: 1986, Scaling of Newtonian and non-Newtonian fluid dynamics without inertia for quantitative modelling of rock flow due to gravity (including the concept of rheological similarity), *Physics of the Earth and Planetary Interiors* **43**(4), 316–330.

Zweigel, P.: 1998, Arcuate accretionary wedge formation at convex plate margin corners: results of sandbox analogue experiments, *Journal of Structural Geology* **20**(12), 1597–1609.